

Large scale circulations and energy transport in contact binaries

K. Stępień^{1*}

¹Warsaw University Observatory, Al. Ujazdowskie 4, 00-478 Warszawa, Poland

Accepted –. Received – ; in original form –

ABSTRACT

A hydrodynamic model for the energy transport between the components of a contact binary is presented. Energy is transported by a large-scale, steady circulation carrying high entropy matter from the primary to secondary component. The circulation is driven by the baroclinic structure of the common envelope, which is a direct consequence of the nonuniform heating at the inner critical Roche lobes due to unequal emergent energy fluxes of the components. The mass stream flowing around the secondary is bound to the equatorial region by the Coriolis forces and its width is determined primarily by the flow velocity. Its bottom is separated from the underlying secondary’s convection zone by a radiative transition layer acting as an insulator. For a typically observed degree of contact the heat capacity of the stream matter is much larger than radiative losses during its flow around the secondary. As a result, its effective temperature and entropy of decrease very little before it returns to the primary. The existence of the stream changes insignificantly specific entropies of both convective envelopes and sizes of the components. Substantial oversize of the secondaries, required by the Roche geometry, cannot be explained in this way. The situation can, however, be explained by assuming that the primary is a main sequence star whereas the secondary is an advanced evolutionary star with hydrogen depleted in its core. Such a configuration is reached past mass transfer with mass ratio reversal. Good agreement with observations is demonstrated by model calculations applied to actual W UMa-type binaries. In particular, a presence of the equatorial bulge moving with a relative velocity of 10-30 kms^{-1} around both components of AW UMa is accounted for.

Key words: stars: contact – stars: eclipsing – stars: binary – stars: evolution

1 INTRODUCTION

Contact binaries have been defined by Kuiper (1941) as binaries with components surrounded by a common envelope. Within the Roche approximation for the total potential in a rotating frame of reference, the envelope lies between the inner and outer critical equipotential surfaces, defined respectively by the Lagrangian points L_1 and L_2 . Cool contact binaries with spectral types later than F0 are called W UMa type binaries (Mochnecki 1981).

W UMa type stars are fairly common in space. Rucinski (2002) estimates that one such binary occurs per 500 main sequence stars in the solar vicinity but these stars do not appear among members of the young and intermediate age clusters. Their occurrence rapidly increases in old open and globular clusters (Kaluzny & Rucinski 1993; Rucinski 1998, 2000). This result indicates that cool contact configurations

are not formed at, or near the zero age main sequence (ZAMS) but at the substantially later age. As it is now commonly assumed, they are formed from initially detached binaries which lose orbital angular momentum (AM) at such a rate that a contact is reached after several Gyr. Kinematically, field W UMa stars belong to old disk, which supports their advanced age (Guinan & Bratstreet 1988; Bilir et al. 2005). The most promising mechanism for AM loss is related to the chromospheric-coronal activity of binary components (Vilhu 1982; Mochnecki 1985; Stępień 1995) although a high incidence of companions to W UMa stars (Rucinski et al. 2007) suggests that a third body may also play a role in orbit tightening (Eggleton & Kiseleva 2001).

Kuiper (1941) noted that a contact binary is stable only when both components are identical. Otherwise, a binary consisting of two stars with the same composition is unstable and mass will be transferred inside the common envelope from the more massive (primary) to the less massive (secondary) component. The transfer is driven by a nonuniform

* e-mail: kst@astrouw.edu.pl

heating of the base of the common envelope due to unequal emergent luminosities at the inner critical surface. By continuity, temperature differences on each equipotential surface above the Roche lobes exist. As a result, the common envelope must be treated as baroclinic rather than barotropic (Shu et al. 1979; Tassoul 1992). Different vertical (i.e. perpendicular to the local equipotential surface) pressure stratifications in both components produce the horizontal pressure gradient driving mass motions on a dynamical time scale. Even if the pressure is constant over a given equipotential surface, a difference appears above and below that surface (Kähler 2004). In the absence of the Coriolis force the resulting large scale flows are symmetric around the axis joining centers of both stars (Webbink 1976). However, for a flow velocity being a significant fraction of the sound velocity the Coriolis force cannot be neglected. The force will deflect the flow towards one side of the throat between the components making it go around the other star in the direction of its orbital motion (see Fig. 4 in Kuiper 1941). Subsequent computations of the streamlines in semidetached binaries confirmed a strong influence of the Coriolis force (see e.g. Lubow & Shu 1975, Lubow & Shu 1976, Oka et al. 2002). When the flow returns to the parent star it is directed to the other side of the throat (Kuiper 1941).

Together with mass, thermal energy is carried to the other component, so we should expect a significant modification of the apparent surface brightness of both stars, compared to a detached binary. Indeed, observations of W UMa type stars show eclipse minima of nearly equal depth indicating almost the same surface brightness of both components. It indicates that, unless mass ratio is close to one, a substantial fraction of the flux radiated by the secondary component comes from the primary.

A very elegant model of a W UMa type binary consisting of two main sequence stars was developed by Lucy (1968, 1976) and Flannery (1976) (see also Yakut & Eggleton 2005 and references therein). The model assumes that each component is out of thermal equilibrium, with a radius oscillating around its critical Roche lobe (inner critical surface). The model requires that matter transported from the primary fully covers the secondary like a hot blanket. The blanket blocks completely the radiation energy flux produced in the core of the secondary. The blocked flux is converted into the thermal energy of the secondary which expands on the stellar thermal time scale. Specific entropy in its convection envelope increases, approaching the value corresponding to the primary's convection zone, which, at the same time, decreases somewhat due to energy transfer. When the expanding secondary overflows its Roche lobe, mass and energy transfer from the primary is stopped and the star shrinks radiating away the excess thermal energy until the cycle of these thermal relaxation oscillations (TRO) repeats. The TRO model successfully explained two important properties of W UMa type stars: an abnormal radius ratio of the components (assumed to be MS stars), required by the Roche geometry, and essentials of the observed light curves.

It will be shown below that, due to the Coriolis force, the stream of matter from the primary is bound to the equatorial belt of the secondary. The polar regions are not covered by the stream so the star can freely radiate away its nuclear energy. As a result, the specific entropy in its convection zone increases insignificantly and remains consider-

ably below the value characteristic of the primary convection zone. Also its radius hardly increases, which excludes MS secondaries oversized by a factor of 2-3 observed in many W UMa stars (Stępień 2006a). Substantially oversized secondaries can, however, be naturally explained by assuming that, instead of being MS objects, they are highly evolved stars with depleted hydrogen in the center or even possessing small helium cores (Paczyński et al. 2007).

A possibility of existing cool contact binaries with secondaries more advanced evolutionary than the primaries has been mentioned in a number of papers (Tapia & Whelan 1975; Sarna & Fedorowa 1989; Eggleton 1996) but such systems were considered to be exceptions from the general rule stating that W UMa stars have not reversed mass ratios. An evolutionary model with mass ratio reversal being a *necessary* condition for forming a W UMa type binary was proposed by Stępień (2004, 2006a,b). The starting configuration for such a model is a close detached binary with a initial orbital period of a couple of days. The binary loses AM via a magnetized wind from both components. The AM loss rate varies approximately as M^{-3} , where M is a stellar mass (Gazeas & Stępień 2008). This dependence is very similar to the mass dependence of the MS evolutionary time scale. Because of this coincidence the primary is expected to be close to, or just beyond terminal age MS (TAMS) at the time when the Roche lobe descends onto its surface. Mass transfer follows in a similar manner as in Algols i. e. with mass ratio reversal. The present primary moves upwards and towards ZAMS in the Hertzsprung-Russell (HR) diagram after receiving hydrogen-rich matter from the present secondary, whereas the secondary becomes substantially oversized for its mass. Each star separately is in thermal equilibrium while filling its critical Roche lobe. Further evolution of the binary is governed by a self-regulating mechanism with two processes acting in the opposite directions: evolutionary expansion of the secondary, followed by mass transfer to the primary, which leads to widening of the orbit and orbital AM loss tightening it. As a result, a contact configuration is maintained with a slow (on a nuclear evolution time scale) net mass transfer from the secondary to primary (Gazeas & Stępień 2008) until coalescence occurs when the mass ratio reaches a critical value (Rasio 1995).

The model explains the Kuiper paradox, i. e. the existence of an equilibrium configuration with component sizes required by the Roche geometry. It does not, however, explain the observed properties of light curves. The energy transport between the components is not a part of that model. It is an independent process which will be considered in detail in the present paper.

The paper is organized as follows: basic assumptions and equations governing the mass and energy flow are given in Sect. 2. The stream structure across and along the flow is discussed in Sect. 3, together with the application of the derived formulas to two actual contact systems. Section 4 describes the global reaction of both components to the circulation and Sect. 5 discusses the results of the paper. It also summarizes main results.

2 EQUATIONS AND ASSUMPTIONS

The basic Eulerian equations of fluid flow in a frame of reference rotating with the binary are:

continuity equation

$$\frac{\partial \rho}{\partial t} + \nabla \cdot (\rho \mathbf{v}) = 0, \quad (1)$$

momentum equation

$$\frac{\partial \mathbf{v}}{\partial t} + (\mathbf{v} \cdot \nabla) \mathbf{v} = \frac{1}{\rho} \nabla p + \nu \nabla^2 \mathbf{v} - \nabla \varphi - 2\boldsymbol{\Omega} \times \mathbf{v}, \quad (2)$$

and entropy equation

$$\rho T \left[\frac{\partial s}{\partial t} + (\mathbf{v} \cdot \nabla) s \right] = -\nabla \cdot \mathbf{F} + d_{\text{visc}}. \quad (3)$$

Here ρ, p, s and \mathbf{v} denote gas density, pressure, entropy and velocity, φ is the gravitational (plus centrifugal) potential, ν is kinematic viscosity coefficient, d_{visc} is the viscous term, \mathbf{F} is the radiative energy flux and $\boldsymbol{\Omega}$ is angular velocity. In the momentum equation the viscous term with $\nabla(\nabla \cdot \mathbf{v})$ has been left out as unimportant (see below).

Assuming that the life-time of the cool contact configuration is of the order of one or more Gyr, we consider a stationary solution of the above set of equations on a time scale longer than the thermal time scale. We put, then, $\partial/\partial t \equiv 0$. We assume that a steady mass flow from the hotter primary to the secondary exists in the common envelope. The assumption of steady motion eliminates any dynamical instabilities, generation of acoustic waves or any other processes taking place on a very short time scale. After leaving the throat between the components the mass stream quickly assumes the azimuthal motion with hydrostatic equilibrium condition in the vertical and meridional directions satisfied.

Let us first consider an inviscid motion. The inertial term on the left hand side of Eq. (2) is of the order of $v^2/l = v^2/2\pi R_{\text{sec}}$, as the flow driving force results from the azimuthal pressure gradient. It can be compared to the Coriolis term of the order of $2\Omega v$. Their ratio is called the Rossby number Ro

$$Ro = \frac{v^2}{2\pi R_{\text{sec}}} / 2\Omega v \approx \frac{v}{4\pi v_{\text{eq}}}, \quad (4)$$

where v_{eq} is the equatorial velocity of a rotating star. In a typical W UMA type star $v_{\text{eq}} \approx 100 - 150 \text{ km s}^{-1}$, so as long as the flow is not highly supersonic $Ro \ll 1$ and we can safely neglect the inertial term. The equation of motion becomes then

$$\frac{1}{\rho} \nabla p = 2\boldsymbol{\Omega} \times \mathbf{v} + \nabla \varphi, \quad (5)$$

where \mathbf{v} has only one, non-vanishing azimuthal component v . The above equation describes the so called geostrophic flow in which the meridional component of the Coriolis force balances the lateral pressure gradient, perpendicular to the direction of motion. Such flows are often observed in the terrestrial atmosphere when air circulates around a high or low pressure center.

3 THE STREAM STRUCTURE

3.1 Lateral equilibrium

We introduce a spherical system of coordinates with the origin at the secondary star center (r, ϑ, ϕ) and we neglect the deviation of equipotential surface shapes from spheres. Because the stream is symmetric relative to the equator, we consider only a hemisphere $0 \leq \vartheta \leq \pi/2$. Far from the throat matter flows along the equator of the secondary in a belt with a half-width $\Delta x = R_{\text{sec}}(\pi/2 - \vartheta_f(r))$, where $\vartheta_f(r)$ is the depth dependent polar angle of the flow boundary. In general, pressure inside the flow is a function of all three coordinates but within our assumptions it is a slowly varying function of the azimuthal direction so it can be assumed constant when considering equilibrium in the radial and meridional direction. The equilibrium condition results from Eq. (5):

meridional component

$$\frac{1}{r} \frac{\partial p}{\partial \vartheta} = 2\rho k c_s \Omega \cos \vartheta, \quad (6)$$

and the radial component

$$\frac{\partial p}{\partial r} = 2\rho k c_s \Omega \sin \vartheta + \rho \frac{d\varphi}{dr}. \quad (7)$$

Eq. (6) can be integrated

$$p(\vartheta) = p_o - 2r\rho k c_s \Omega (1 - \sin \vartheta), \quad (8)$$

where p_o is the pressure at the equator. The ambient pressure under the secondary's photosphere is equal to p_{sec} , so the boundary will be reached when $p(\vartheta_f) = p_{\text{sec}}$. This gives a condition for ϑ_f

$$\sin \vartheta_f = 1 - \frac{p_o - p_{\text{sec}}}{2\rho k c_s v_{\text{eq}}}. \quad (9)$$

Above the photosphere $p_{\text{sec}} \equiv 0$. With a total thickness $\Delta r \ll R_{\text{sec}}$ the stream layer is thin, so we can replace coordinate r appearing explicitly in Eq. (8) by R_{sec} .

Viscosity will produce a drift of the stream matter into high astrophysical latitudes. Molecular viscosity is negligibly small but the convective viscosity may play a role. We can estimate a possible drift resulting from that viscosity

$$\nu = \frac{1}{3} l_{\text{conv}} v_{\text{conv}}, \quad (10)$$

where l_{conv} and v_{conv} are the mixing length and convective velocity near the bottom of the stream.

Assuming that l_{conv} is of the order of pressure scale height near the bottom of the flow one obtains from the model of the convective zone $H_p \approx 10^9 \text{ cm}$ and $v_{\text{conv}} \approx 2 \times 10^4 \text{ cm s}^{-1}$ so $\nu \approx 7 \times 10^{12}$ in cgs units (Baker & Temesvary 1966; Spruit 1974). The resulting viscous term in the momentum equation is of the order of $\nu v / \Delta x^2$. For $v \approx 0.3c_s$ and $\Delta x \approx R_{\text{sec}}/2$ this term is equal to $2 \times 10^{-2} \text{ cm s}^{-2}$. It takes about 3 d for a given flow element to encircle the secondary assuming a typical flow velocity about 10 times slower than v_{eq} , see below. The total drift distance of the stream in the meridional direction is equal then to $\sim 2 \times 10^3 \text{ km}$ which is completely negligible compared to the stream width. We conclude that viscosity can be neglected altogether when considering dynamics of the mass flow around the secondary.

3.2 Vertical equilibrium

A typical W UMa type binary consists of two unequal mass components possessing convective envelopes. Except for stars with spectral type around F0 where the convection zone is very thin and mostly super-adiabatic, its dominant part is stratified nearly adiabatically i. e. according to the pressure-temperature relation

$$p = KT^\alpha, \quad (11)$$

where $\alpha = 2.5$ for fully ionized gas and $K = \text{const.}$ throughout the considered part of the convection zone. The parameter K is called the adiabatic constant and its value depends on the specific entropy of the matter in the convection zone. Realistic models of the convection envelope take into account all important effects influencing its stratification, like variability with depth of K, α , and specific heats as well as deviations from strict adiabaticity (Baker & Temesvary 1966; Spruit 1974). However, most of these effects take place in the uppermost layers of the convection zone where the pressure is low. Because we are interested in the pressure equilibrium at some depth below the stellar surface, a detailed structure of these shallow layers is unimportant. As the accurate models of the convection zone of solar type stars indicate, the stratification becomes very close to adiabatic already for temperatures higher than about 10^4 K. We adopt the adiabatic stratification for the convective envelopes of both components with different values of the adiabatic constant.

Matter flowing from the primary is characterized by the same adiabatic constant K_{pr} as the convection layer of the primary. The convection layer of the secondary is described by K_{sec} . In general, $K_{\text{sec}} < K_{\text{pr}}$. Figure 1 gives an example of two pressure-temperature relations corresponding to two adiabatic constants differing by 0.5dex. The upper line on each diagram gives the $p-T$ relation for the stream and the lower line for the ambient convection layer of the secondary.

Vertical hydrostatic equilibrium condition requires continuity of the pressure at the boundary between the stream and the underlying convective layer not affected by the flow. Because the secondary convection zone has specific entropy lower than the stream, a discontinuity in entropy and temperature must occur at this boundary (a vertical segment of the solid line in Fig. 1 top). A steady state model with a contact discontinuity of this kind was considered by Shu et al. (1976, 1979). They assumed that matter streaming from the primary fully covers the secondary component of a contact binary. They tried to build a model in which the nuclear energy of the secondary can flow outwards in spite of the discontinuity. Hazlehurst & Refsdal (1978) argued, however, that such a model contradicts the second law of thermodynamics because the nuclear energy of the secondary cannot flow from the low to the high entropy medium above. Instead, the nuclear energy will heat the convection zone on a thermal time scale rising its specific entropy to the value characteristic of the blanketing matter, just as assumed in the TRO model.

The situation considered in the present paper is, however, entirely different. The streaming matter covers now only a part of the secondary. There is no need to introduce a contact discontinuity. The hot stream matter heats the layer lying underneath and lowers the temperature gradient

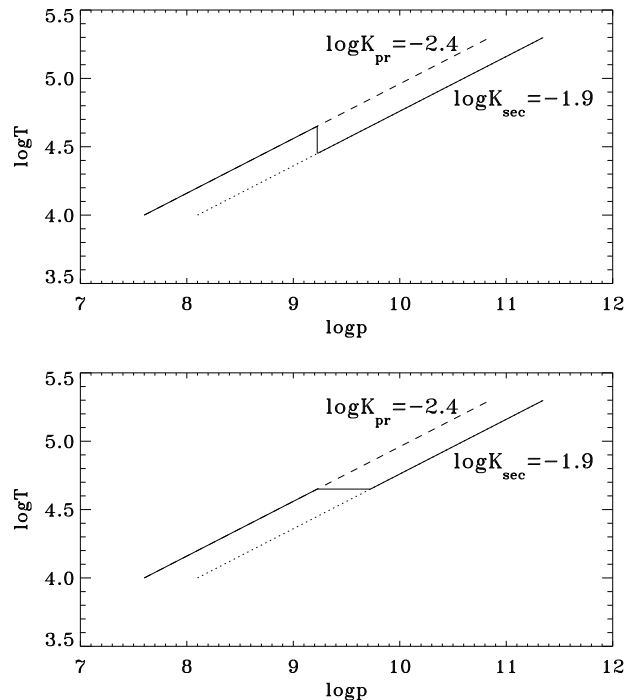


Figure 1. The adiabatic $p-T$ relations for the stream matter (upper lines) and the secondary's convection zone (lower lines). The condition of the continuous pressure across the contact surface between the stream and the unaffected convective layer beneath requires a temperature discontinuity (a solid line, top). The formation of a radiative transition layer with a flat temperature gradient between the stream and the deeper unaffected layers results in a continuous transition both in pressure and temperature (a solid line, bottom).

there. As a result, the convective energy flow from below is inhibited. In steady state a radiative layer is formed with a low temperature gradient and specific entropy increasing outwards from the value characteristic of the secondary convection zone up to the value characteristic of the stream gas. We will call it a transition layer. Such a layer with the temperature gradient equal to zero is shown in Fig. 1 (bottom) as a horizontal segment of the solid line. In real stars the gradient will probably be not equal exactly to zero so the transition layer will be thicker than shown. The heat transport is completely, or nearly completely, blocked in the transition layer which acts as an insulator. The energy blocked by the stream will be redistributed over the whole convection zone of the secondary and ultimately radiated away from the polar regions not covered by the stream matter (see Section 4).

To consider the vertical structure of the stream in more detail we need to calculate $p_o - p_{\text{sec}}$ with depth. Because the depth of the layers in question is much lower than the stellar radius we can use the plane parallel approximation with the coordinate z replacing r . Let us assume that the secondary convection zone remains unaffected by the stream below the bottom of the transition layer and we put the reference level $z = 0$ there. The pressure is constant over the whole equipotential surface lying at that level. We denote it

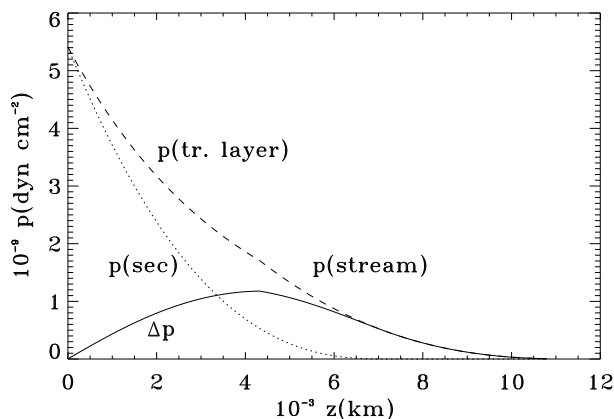


Figure 2. The vertical pressure distribution across the stream together with the transition layer (broken line), in the unperturbed secondary convection zone (dotted line) and their difference (solid line), balanced by the meridional component of the Coriolis force (see text). The bottom of the transition layer is at $z = 0$ and the bottom of the stream (expected to coincide with the Roche critical surface) is at $z \approx 4 \times 10^3$ km.

by p_b . Within the isothermal transition layer pressure varies as

$$p(z) = p_b \exp(-z/H_p), \quad H_p = \frac{k_B T_o}{\mu H g_{\text{eff}}}, \quad 0 \leq z \leq z_o, \quad (12)$$

where μ is the mean molecular weight, H – mass of the hydrogen atom, k_B – the Boltzmann constant, T_o – temperature of the layer, g_{eff} – the effective gravity and z_o corresponds to the bottom of the stream, which agrees with the top of the transition layer. The pressure is continuous at the interface between the transition layer and the adiabatically stratified stream where temperature varies as

$$T(z) = T_o - \frac{g_{\text{eff}}}{c_p}(z - z_o), \quad z \geq z_o, \quad (13)$$

where c_p is specific heat at constant pressure. When calculating the $T(z)$ relation we neglect variability of the effective gravity. With $T(z)$ known, the vertical pressure stratification is obtained from Eq. (11) where $K = K_{\text{str}}$. As it will be shown below, the entropy of the stream matter varies very little during the flow around the secondary, so we can put $K_{\text{str}} \approx K_{\text{pr}}$ everywhere.

It is reasonable to assume that in steady state the transition layer will be partially dragged by the stream in such a manner that a gas layer lying immediately below the stream moves with a stream velocity and deeper layers move slower until zero velocity is attained at the bottom of the transition layer. We arbitrarily assume that velocity inside the transition layer varies as

$$v(z) = k c_s \frac{\rho_b - \rho(z)}{\rho_b - \rho_t}, \quad (14)$$

where ρ_b and ρ_t are the densities at the bottom and at the top of the transition layer. Thus defined velocity vanishes at the bottom and reaches the stream velocity at the top.

Far from the stream the convection zone of the secondary remains unperturbed with the adiabatic stratification. Neglecting a difference between c_p in the stream and in the ambient convection zone we have

$$T(z) = T_o - \frac{g_{\text{eff}}}{c_p} z, \quad (15)$$

Pressure stratification is obtained again from Eq. (11), except that now $K = K_{\text{sec}}$.

Figure 2 shows an example of the vertical pressure distribution inside the transition layer and the stream with depth equal to 1 % of the primary's radius (broken line), in the unperturbed secondary convection zone (dotted line) and their difference (solid line). As it is seen from the figure, the stream extends above the surface of the secondary and produces an equatorial bulge held by the meridional component of the Coriolis force (see also Fig. 3).

3.3 The thermal stream structure along the flow

With the depth and width of the stream specified, the mass transfer rate F_p can be calculated

$$F_p = 2\Delta x \int_0^{\Delta r} k c_s \rho dr = 2\Delta x k c_s \overline{M}_{\Delta r}, \quad (16)$$

where $\overline{M}_{\Delta r}$ is the column mass above the level Δr . The stream also carries thermal energy which is partly radiated away during its flow around the secondary. We will now discuss the variation of the stream thermal structure along the flow.

Let us consider a slice of matter perpendicular to the flow with thickness $R_{\text{sec}} d\phi$. Its total heat (internal energy plus enthalpy) capacity dQ is equal to

$$dQ = 2\Delta x R_{\text{sec}} d\phi \int_0^{\Delta r} \rho c_p T dr = 2\Delta x R_{\text{sec}} c_p \overline{MT}_{\Delta r} d\phi, \quad (17)$$

where

$$\overline{MT}_{\Delta r} = \int_0^{\Delta r} \rho T dr. \quad (18)$$

The matter flowing around the secondary radiates energy at a rate σT_{str}^4 per unit time and area, where T_{str} is the effective temperature of the stream. In general, T_{str} will decrease along the flow from its initial value, assumed to be close to the effective temperature of the primary, T_{pr} , and its precise variation could be determined by solving the transfer equation within the stream. To avoid cumbersome calculations we discuss two limiting cases: first, when the total heat capacity of the stream is much higher than the total energy radiated away, and then, when the heat capacity is comparable to the radiated energy.

The slice has a radiating area $2\Delta x R_{\text{sec}} d\phi$ and emits $dF_{\text{rad}} = 2\sigma T_{\text{str}}^4 \Delta x R_{\text{sec}} d\phi$ energy per unit time. It takes a time equal to $2\pi R_{\text{sec}}/k c_s$ to encircle the secondary. The total energy radiated away during this time is

$$dL = \frac{4\pi\sigma T_{\text{str}}^4 \Delta x R_{\text{sec}}^2 d\phi}{k c_s}. \quad (19)$$

From Eqs. (17) and (19), the limiting case of large heat capacity, $dQ \gg dL$, corresponds to the condition

$$c_p \overline{MT}_{\Delta r} \gg \frac{2\pi\sigma T_{\text{pr}}^4 R_{\text{sec}}}{k c_s}. \quad (20)$$

If the radiated energy is small compared to the total heat capacity of the stream, its effective temperature will change very little from its initial value T_{pr} so we can put

$T_{\text{str}} \approx T_{\text{pr}}$. In case of low heat capacity the effective temperature of the stream will approach the effective temperature of the secondary and the stream matter will mix together with its convection zone.

Assuming that the energy outflow from the stream influences uniformly its entropy, i. e. that the stream specific entropy is constant with depth, we can calculate its decrease from Eq. (3). In case of the large heat capacity we obtain

$$\Delta s = -\frac{4\pi R_{\text{sec}} \sigma T_{\text{pr}}^4}{k c_s \overline{MT}_{\Delta r}}. \quad (21)$$

In case of the low heat content, T_{pr} in Eq. (21) should be replaced by the properly defined average stream effective temperature.

The entropy decrease can be compared with entropy of the primary convection zone

$$s_{\text{pr}} = -\frac{k}{\mu H} \ln K_{\text{pr}}. \quad (22)$$

After return to the primary, the stream matter sinks in its convection zone.

3.4 Numerical example: AB And

To obtain a numerical estimate of the parameters describing an actual stream in a cool contact binary we apply the above derived equations to a typical W-type contact binary. As an example, we take AB And. It has the orbital period $P_{\text{orb}} = 0.33$ d, component masses $M_{\text{pr}} = 1.04 M_{\odot}$ and $M_{\text{sec}} = 0.60 M_{\odot}$, and volume radii $R_{\text{pr}} = 1.02 R_{\odot}$ and $R_{\text{sec}} = 0.78 R_{\odot}$ (Baran et al. 2004). These data give $v_{\text{eq}} = 120 \text{ km s}^{-1}$ for the secondary component. The star has a relatively low fill-out factor $f = 0.05$ (Baran et al. 2004), which corresponds to about 1 % of the primary star radius. Assuming that the equal pressure equipotential surface is close to the inner critical Roche lobe we obtain $\Delta r \approx 0.01$ for the depth of the stream. The sound velocity is equal to 30 km s^{-1} at this depth. The width of the stream can be calculated from Eq. (9). Figure 3 shows the results. Here the angular half-width is plotted as an abscissa for different heights above the bottom of the transition layer. The broken heavy line on the right indicates the approximate photospheric level of the secondary. The diagrams give the stream width for three values of $\Delta r/R_{\text{pr}}$ equal to 0.005 (top), 0.01 (middle) and 0.03 (bottom) and three values of k , as indicated. The width was calculated up to the level where temperature reached 10 000 K because for lower temperatures the adiabatic model breaks down. As we see, the largest width of the stream is close to the photosphere of the secondary but the Coriolis force produces a bulge above the stellar equator with a height of the order of the stream depth. As expected, a lower stream velocity results in its increased width and in the limit of zero velocity the stream would cover the whole secondary. For flow velocities comparable to the sound velocity, i. e. for k between 1 and 0.3, the stream has a half-width between 15° and 30° (Fig. 3), and covers between $1/4$ and $1/2$ of the stellar surface, respectively.

A schematic side view of AB And with a stream covering 50 % of the secondary's surface is shown in Fig. 4.

The stream with a depth of 0.01 carries enough mass and energy to be in the regime of large heat capacity. To

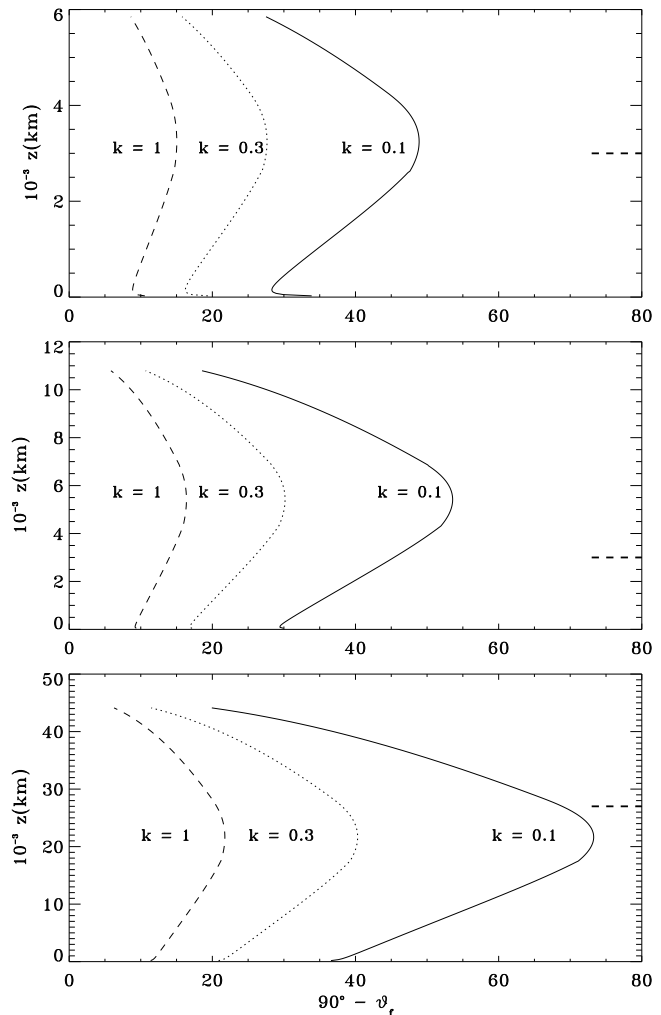


Figure 3. The width of the stream as a function of height above the bottom of the transition layer for three values of k describing the ratio of stream to sound velocity and for three depths of the stream: 0.5 % (top), 1 % (middle) and 3 % (bottom) of the primary's radius. A broken heavy line on the right indicates an approximate level of the secondary's photosphere. Note a weak dependence of the stream width on its total depth.

see it we substitute the following values to Eqs. (17) and (20): $\Delta r = 7 \times 10^{10}$ cm, $\bar{c}_p = 10^9$ (in cgs units), $T_{\text{pr}} = 5590$ K (see next section) and $k = 0.3$. The column mass and the integral $\overline{MT}_{\Delta r}$ are calculated from the convection zone model. We obtain $\overline{M}_{\Delta r} = 3.5 \times 10^5 \text{ g cm}^{-2}$ and $\overline{MT}_{\Delta r} = 1.7 \times 10^{10} \text{ g K cm}^{-2}$. The resulting mass transfer rate is $F_p = 5 \times 10^{-4} M_{\odot}/\text{year}$. The left hand side of Eq. (19) gives 1.7×10^{19} (in cgs units) and the right hand side gives 4×10^{16} in the same units. The resulting ratio of both numbers is equal to 2.4×10^{-3} which indicates that the non-equality given by Eq. (19) is very well fulfilled. The numbers become comparable only for stream depths less than 0.5 % of the stellar radius. Figure 3 (top) shows the calculated width of the stream with the depth of 0.5 %. It is somewhat surprising that its width is not much different from the widths of much more massive streams shown in Fig. 3 (middle) and (bottom). It is clear that only extremely marginally contact binaries with overfill factors not exceeding a couple

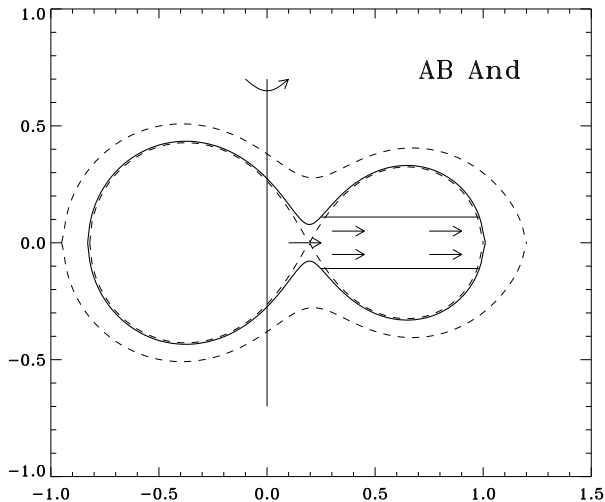


Figure 4. A side view of AB And with a stream covering a half of its surface. Broken lines indicate inner and outer critical surfaces and the solid line shows the binary surface.

of hundredths will have streams with surface temperature approaching the temperature of the uncovered part of the secondary component.

The change of specific entropy of the stream in AB And can be calculated from Eq. (20). With the adopted parameters we obtain $\Delta s = -1.2 \times 10^6 \text{ ergg}^{-1}\text{K}^{-1}$. According to Eq. (21) its initial specific entropy is equal to 4.59×10^8 in the same units so the decrease of entropy during the flow around the secondary is small indeed. It is possible then that the stream returning to the primary component will not sink immediately after passing the throat but it may move over a substantial fraction of the primary's circumference before it plunges in the convection zone.

To summarize, we see that the Coriolis force confines the near sonic stream to the equatorial belt of width $\pm(15^\circ - 30^\circ)$ around the secondary. The stream covers 25-50 % of the stellar surface. For a primary overflowing its Roche lobe by $\sim 1\%$ or more the stream radiates a very small fraction of its total heat capacity which results in its nearly constant surface temperature equal to the primary's temperature. Substantially shallower streams, possible in contact binaries with an extremely marginal contact, will show a temperature decrease from the initial value close to the primary's temperature on the trailing hemisphere of the secondary, down to the value close to the secondary's temperature on the leading hemisphere of the star.

After return to the primary, the stream will sink in its convection zone due to the lower entropy. The Coriolis force deflects the returning stream to the opposite side of the throat, compared to the stream flowing towards the secondary. The deflection should reduce an interaction of both flows although it will not separate them completely. The returning flow will collide with matter streaming towards the throat (see Figs. 1 and 2 in Oka et al. 2002). However, the collision will not be head-on, as obtained by Martin & Davey (1995) who simulated a two dimensional motion in an equatorial plane of a contact binary. Geometry applied by the authors prevents matter from crossing the plane containing

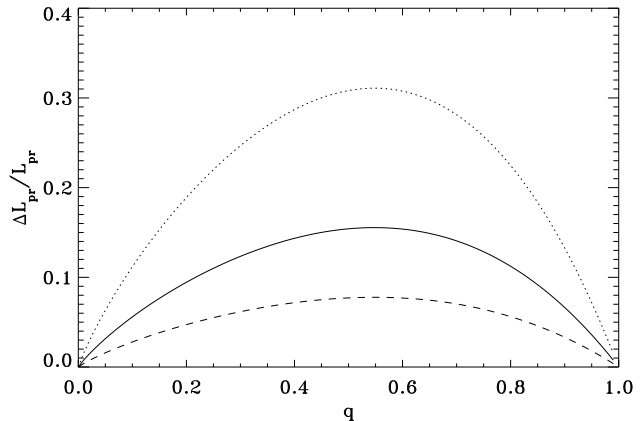


Figure 5. A fraction of the primary component luminosity radiated away by the stream flowing around the secondary component as a function of mass ratio. The curves correspond to three values of coverage of the secondary by the stream: full coverage (dotted line), half-coverage (solid line) and quarter-coverage (broken line).

centers of both stars and the rotation axis, so the stream cannot move to one side of the throat, as shown by three dimensional calculations (Oka et al. 2002).

4 GLOBAL REACTION OF THE BINARY TO THE MASS AND ENERGY FLOW

4.1 The influence of the stream

As it was mentioned earlier, the stream acts like a hot blanket covering part of the secondary and blocking the energy flow from below by rising the temperature of the layer immediately beneath. As a result, a transition radiative layer is formed with a decreased temperature gradient in which the specific entropy increases from the bottom value characteristic of the secondary convection zone to the top value characteristic of the stream.

What is the global reaction of a star when a fraction of its surface cannot radiate away the stellar core energy due to an obstacle blocking the energy outflow? The physical nature of the obstacle is not so important as long as it occurs in the outermost stellar layers. One example of such an obstacle partly blocking the energy flow from below is a dark starspot appearing on the surface of an active star. Another example can be seen in close binaries when a hot companion irradiates a part of the surface of a cool component. Both effects have been discussed at length in the literature (e. g. Ritter et al. 2000, Spruit & Weiss 1986 and references therein). The blocked energy flux is redistributed inside the convection zone and re-radiated by the unperturbed part of the stellar surface. The detailed models show that the specific entropy of the convection zone is somewhat increased and so is the stellar radius. For stars with deep convection zones, or fully convective, the nuclear energy production may also be affected. Assuming a steady state in which a constant fraction of the stellar surface is covered by spots over a time long compared to the thermal time scale of the convection zone, Spruit & Weiss (1986) obtained the following expression for the equilibrium stellar radius

$$R_e(f_{ps}) = R_o(1 - f_{ps})^d, \quad (23)$$

where R_e and R_o denote the equilibrium radius of the spotted and unspotted star, f_{ps} is the fraction of the stellar surface permanently covered by spots and $d \approx -0.1$. An essentially identical expression was found by Ritter et al. (2000) for stars irradiated by hot companions. For $f_{ps} = 0.25$ and 0.5 the equation gives $R_e = 1.03R_o$ and $1.07R_o$, respectively. In stars with not too deep convection zones the nuclear energy production remains unaffected. The reduction of the effective radiating surface is exactly compensated by an increase in surface temperature of the undisturbed part of the star

$$T_{\text{eff}}^e = (1 - f_{ps})^{-\frac{1+d}{4}} T_{\text{eff}}, \quad (24)$$

where T_{eff}^e and T_{eff} are the equilibrium and undisturbed effective temperature. More accurate values of the equilibrium radius and temperature depend on stellar mass (Spruit & Weiss 1986).

The primary component suffers from additional cooling of its surface by the stream encircling the secondary. The stream feeds the primary with the lower entropy matter which is mixed with the rest of its convection layer. As a result, the specific entropy of the convection zone is somewhat lowered and so is the stellar radius but the expected changes should be close to those occurring in the secondary component, i.e. they should not exceed one, or at most a few percent. The primary, slightly undersized for its mass, will appear closer to ZAMS in the HR diagram. Neglecting its radius change we can obtain the modified effective temperature of the primary

$$T_{\text{pr}}^m = \left(1 - \frac{\Delta L_{\text{pr}}}{L_{\text{pr}}}\right), \quad (25)$$

where L_{pr} is the luminosity of the primary component and ΔL_{pr} is a fraction of this luminosity radiated away by the stream flowing around the secondary component (Fig. 5).

Now let us calculate the expected values of the thermal parameters of AB And. The effective temperature of a single one solar mass star is about 5800 K. That should be close to the temperature of the undisturbed primary. Assuming that secondaries of W UMa type stars are evolved stars with hydrogen depleted in their stellar cores (Stępień 2004, 2006a) we obtain the following values of the global parameters for the unperturbed secondary of AB And: $T_{\text{eff}} = 4570$ K, and $L/L_{\odot} = 0.24$. The data were taken from the evolutionary models of stars with masses equal to the present masses of the secondaries.¹ This is not fully consistent with the present considerations because, according to the accepted model, the secondaries were originally more massive and their present masses result from mass exchange. It is hoped, however, that differences between the adopted and fully consistent models are of secondary importance. Let us assume, as an example, that the stream covers 50% of the secondary and that its nuclear energy production rate is unaffected by this. According to Eq. (23) the steady state effective temperature of the surface fraction not covered by

the stream rises to 5340 K. The primary transfers about 16% of its luminosity (see Fig. 5) to the secondary so its actual effective temperature, resulting from Eq. (25), drops to 5590 K. The effective temperature of the stream is of course the same. The “final” surface averaged temperature of the secondary is equal to about 5480 K, which is nearly identical as obtained by Baran et al. (2004) from observations who give $T_{\text{sec}} = 5500$ K. However, the observed primary’s temperature equal to 5140 K is substantially lower than resulting from the present model. A possible explanation of this discrepancy is discussed in the next Section.

4.2 The W-type phenomenon and photospheric starspots

The observed temperatures of components of a W UMa type binary belong to the least accurately determined stellar parameters (Yakut & Eggleton 2005). The primary’s temperature is usually determined from the spectral type which is uncertain due to very broad spectral lines, or from the photometric index. It is kept constant during the light curve modeling. The secondary’s temperature results from modeling of the light curve, in particular from the relative depth of both minima, which gives a ratio of both temperatures. Such an analysis gives only a rough estimate of the surface averaged temperatures and is insensitive to their possible variations across the stellar surface. Regarding the relative temperatures of the components, cool contact binaries are divided into two types: W-type when secondaries are hotter than primaries and A-type when the opposite takes place (Binnendijk 1970). A typical temperature difference between the components of genuine contact binaries is of the order of a few hundred kelvin (Yakut & Eggleton 2005). A few stars alternating between W-type and A-type are known with a temperature difference always staying close to zero. The present model gives $\Delta T = T_{\text{pr}} - T_{\text{sec}}$ equal to 110 K for AB And. Several A-type stars are known with ΔT close to this value. However, AB And is of W-type and this phenomenon cannot be explained within the energy transfer mechanism alone. No such mechanism, obeying basic laws of physics, can transfer energy from cooler to hotter medium in an isolated system. So, the most popular explanation of the W-type phenomenon assumes that dark, cool spots cover a substantial fraction of the primary’s surface. The temperature of its spot-free part may be higher than the secondary’s temperature but the apparent surface averaged temperature is lower. W UMa-type stars have a very high level of chromospheric-coronal activity (Cruddace & Dupree 1984; Rucinski 1985; Vilhu & Walter 1987; Stępień et al. 2001) and variations of the light curve, observed on time scales of decades, indicate that they also possess dark starspots covering a variable fraction of the stellar surface. Perhaps the most extreme example of light curve variability due to a variable coverage by spots can be seen in Rucinski & Paczynski (2002).

We can estimate what should be the fraction of the primary’s surface covered by dark spots to lower its average temperature to a required value. Assuming, for simplicity, that umbrae have the surface brightness of 1/4 of the undisturbed photosphere (it is so in the solar case) and that they dominate the spots we have

¹ I thank Dr. Ryszard Sienkiewicz for calculating a set of evolutionary models of low mass stars. The description of his program can be found in Paczyński et al. (2007).

$$T_{\text{pr}}^{\text{f}} = (1 - 0.75f_s)^{1/4}T_{\text{pr}}, \quad (26)$$

where T_{pr}^{f} is the “final” primary’s temperature modified by spots and f_s is the spot coverage. It is assumed here that spots appear and disappear on a time scale short compared to the thermal time scale of the convection zone. When the spots appear, they simply block the respective energy flux which does not reappear elsewhere. In other words, we consider now only the variable component of the spot coverage. If there also exists a permanent spot component covering f_{ps} of the primary’s surface it will influence the effective temperature as discussed above.

For $f_s = 0.25$ we obtain $T_{\text{pr}}^{\text{f}} = 5310$ K, hence $\Delta T = -170$ K. When f_s is increased to 0.5, we obtain $T_{\text{pr}}^{\text{f}} = 4970$ K, hence $\Delta T = -510$ K. This should be compared with the observed value $\Delta T = -340$ K. As we see, the required spot coverage is quite high but reasonable. We know a number of single, rapidly rotating stars with a variable spot coverage within this range, e. g. AB Dor (Innis et al. 2008) or BO Mic (Wolter et al. 2008). Heavily spotted are also cool detached binaries with periods shorter than one day, like XY UMa (Pribulla et al. 2001) or BI Cet (Cutispoto et al. 2003).

The absolute magnitude of AB And, obtained from the visual magnitude and the distance is equal to 4.05 mag (Rucinski & Duerbeck 1997). With $BC = -0.08$ mag (Allen 1973) the binary has the luminosity $L \approx 1.6L_{\odot}$. Adopting $L \approx 1.16L_{\odot}$ for the MS primary of AB And and $L \approx 0.25L_{\odot}$ (see above) for the evolved secondary we obtain $1.4L_{\odot}$ for the total luminosity of the binary. This is less than observed but the difference is not large and can be due to observational uncertainties. Note that if the secondary were a normal MS star, its core luminosity would be close to $0.1L_{\odot}$ which increases the discrepancy with observations.

4.3 The case of AW UMa

Up to recently the spectroscopic observations of contact binaries were not accurate enough to resolve an additional flow on a rapidly rotating component. Excellent observations obtained in the last years by S. M. Rucinski and his group changed the situation. Pribulla & Rucinski (2008) analyzed very accurate profiles of spectral lines of AW UMa – an A-type contact binary with an extreme mass ratio. The observations indicate the existence of an equatorial bulge on both components, moving with velocity 20-30 km/s relative to the rotating frame of reference. The present model predicts such a bulge on the secondary star. Although dynamics of the returning stream was not considered in the present paper it was argued that the returning flow may travel a significant fraction of the circumference of the primary before it disappears beneath the stellar surface. The returning flow, together with the stream formed on the leading hemisphere of the primary, will produce a spectral feature similar to signature of an equatorial bulge.

The observations by Pribulla & Rucinski (2008) showed in addition that parts of the line profiles formed away from the equatorial regions of AW UMa are too narrow for the rigidly rotating components filling the Roche lobes. The authors suggest that the components may be undersized by about 15 percent. However, another explanation is also possible. The flow pattern obtained by Oka et al. (2002) from hydrodynamic simulations of a semi-detached binary shows

the presence of giant eddies surrounding the poles of the donor and rotating contrary to the orbital motion (i. e. contrary to the direction of the stream). Such eddies *reduce* rotational broadening of lines formed in the polar regions. In a contact binary similar eddies may also occur on the secondary. If so, the observed profiles mimic rigid rotation of undersized stars.

Pribulla & Rucinski (2008) stress, however, that such profiles are not common and are not observed e. g. in another contact binary, V556 Oph, in which the spectroscopic observations are in agreement with a conventional contact model. The difference between line profiles observed in AW UMa and V556 Oph may result from a different evolutionary status of both stars and different size of the stream. The secondary component of AW UMa is very likely to be a highly evolved star with massive helium core and a very tenuous envelope (Paczyński et al. 2007). The evolutionary computations suggest that the size of the secondary may be close to its maximum, or even past it, so the secondary may presently undergo evolutionary shrinking. In such a case, the stream can be more massive and move faster than in other binaries in which secondaries still expand due to evolutionary effects. A contact configuration of AW UMa may still be sustained by a slow (net) mass transfer from the primary to the secondary. This transfer results in a shortening of orbital period i. e. it acts in the same direction as AML. The situation when two operating mechanisms tighten the orbit cannot last for long. If so, AW UMa is in an exceptional evolutionary state just prior to final merging of both components. It would be very interesting to identify other stars with properties similar to AW UMa. Secondaries with little or no helium core expand as they evolve. A self-regulating mechanism works in such binaries (Gazeas & Stepień 2008). The expanding secondary transfers mass to the primary on an evolutionary time scale. Mass transfer from a less massive to a more massive component widens the orbit. At the same time, AML tightens the orbit on approximately the same time scale. The whole process contains a negative feed-back: too fast secondary expansion results in an increased mass transfer, which leads in turn to an appropriate widening of the orbit (in spite of AML) and the Roche lobe increase. The Roche lobe of the secondary approaches its surface and the mass transfer is cut down. If, for some reason, the expansion rate of the secondary becomes low, the orbit tightens due to AML, the Roche lobe shrinks and the higher mass transfer rate is restored. Similarly, if AML significantly increases (decreases), the Roche lobe varies correspondingly so that mass transfer rate increases (decreases), resulting in an orbit which is almost insensitive to such fluctuations. V556 Oph and many other W UMa type stars are very likely in such an evolutionary state. Their streams will be less violent and not so contrasted as in case of AW UMa.

5 SUMMARY AND DISCUSSION

5.1 The essentials of the circulation model

It was shown by Stepień (2004, 2006a,b) that an evolutionary model of a cool contact binary in which the primary component is a MS star and the secondary component is an advanced evolutionary star with a hydrogen depleted core

fulfills simultaneously two conditions: both components are in thermal equilibrium and their sizes conform to the geometrical requirement of the Roche model. Energy exchange between the components was not a part of that model. The present paper considers the problem of the energy transport.

A common envelope of a contact binary with unequal components cannot achieve hydrostatic equilibrium. Unequal heating from below of the base of the common envelope by the emergent energy fluxes of the components produces temperature difference on each equipotential surface. A resulting baroclinic structure in the common envelope drives large scale mass motions between the components on a dynamical time scale. Because the stream transports thermal energy together with mass, stellar luminosities are redistributed over the common surface.

Three dimensional hydrodynamic simulations of the mass loss in a semi-detached binary demonstrate that a stream leaving the donor star is deflected by the Coriolis force in the direction of the orbital motion so that matter flows at an angle of about 10° to the line joining star centers. The speed of the stream reaches sound speed already in the vicinity of L_1 point (Lubow & Shu 1975; Oka et al. 2002). After leaving the L_1 region the stream moves down the potential well. If the companion is compact enough, the stream misses its surface, encircles it and forms a disc. If a radius of the companion is larger than a certain critical value, the stream hits its surface. The subsequent stream motion is restricted to two dimensions along the stellar surface. A contact configuration is an extreme case of a large companion filling the same equipotential surface as the donor. The stream is then forced to move from the beginning along the common equipotential surface, to encircle the other component and to return to donor. The same Coriolis force which deflects the stream, prevents it now from spreading up to the stellar poles. Even in the presence of turbulent viscosity the spreading is insignificant. The stream flows in an equatorial belt with the width determined by the stream velocity. Its part is raised above the photosphere and forms an equatorial bulge with height comparable to the stream depth.

Assuming that the bottom of the stream is close to the inner critical Roche surface we can calculate the global parameters of the flow. Typical overflow factors of the W UMa type binaries correspond to thickness of the common envelope of the order of one or a few percent of the stellar radius (Yakut & Eggleton 2005). For the stream depth of one percent and velocity close to the sound speed the stream has a total width of 30° - 60° and carries about $5 \times 10^{-4} M_\odot$ /year with velocity of 10-30 km/s. Its heat capacity is a few orders of magnitude higher than the energy radiated away during the flow around the secondary. As a result, the effective temperature of the stream and its specific entropy decrease very little when it returns to the primary. The returning flow may travel a significant fraction of the stellar circumference before it sinks. Only binaries with an extremely marginal contact in which the common envelope is thinner than about 0.5 percent of the stellar radius have streams with heat capacity comparable to the energy radiated away. The effective temperature and specific entropy of such a stream approach the ambient temperature and entropy of the secondary's convection zone.

The stream covering a fraction of the secondary modifies its thermal structure. It heats the matter immediately

beneath reducing the temperature gradient. The reduced gradient effectively blocks the energy flow from below. A similar situation occurs in stars covered by dark spots or irradiated by a hot companion. The blocked energy is redistributed inside the convection zone and radiated away by the polar regions not covered by the stream. The effective temperature of these regions rises accordingly but the stellar radius hardly changes. Numerical examples show that the surface averaged temperatures of both components are close to one another as observed in contact binaries but the calculated primary's temperature cannot be lower than the secondary's. This is a known result; mass and energy transfer between the component cannot by itself result in the secondary's temperature higher than the primary's. The existence of A-type binaries can be explained solely by large scale circulations but not W-type. As has been suggested many times in the past, large dark spots appearing temporarily on the primary can explain its low surface averaged temperature. Numerical estimates obtained in the present paper indicate that a substantial fraction of the star (25-50 percent) must be covered with spots to lower the temperature by several hundred degrees, required by observations.

5.2 Discussion

Dynamics of the mass transfer between the components of a contact binary, considered in the present paper, is similar to the one investigated by Tassoul (1992). The driving force of the circulations discussed by Tassoul (1992) comes also from the baroclinic structure of the common envelope and the flow is influenced by the Coriolis force. The author applied, however, a different boundary condition at the stellar surface. Based on the observations available at that time he adopted zero velocity and the strictly uniform temperature on the stellar surface of the secondary. Yet more recent observations show the existence of massive flows in some of the W UMa type stars (Pribulla & Rucinski 2008). On the other hand, very little is known about the temperature distribution over the surfaces of both components although nonuniformities in their surface brightness are notoriously invoked to explain the observed light curves (e. g. Gazeas et al. 2006).

Yakut & Eggleton (2005) called attention to a possible role of lateral energy transfer connected with differential rotation observed on the Sun and solar-type stars. Differential rotation results from a coupling between rotation and turbulent convection in an axially symmetric star. AM is transported in the meridional direction by Reynolds stresses, meridional circulations and viscous diffusion (Brown et al. 2008). The mechanism considered in the present paper is different from that. The differential rotation was not included. Nevertheless, it may play a role in forming a stream which transfers mass and energy between the components although more elaborated model of the meridional AM transport in a contact binary is needed.

W UMa type stars show often period variations (Kreiner et al. 2001). Systematic changes with values up to $P = \pm(10^{-6} - 10^{-7})$ day/year have been detected in several stars and interpreted as a signature of TRO. However, recent observations of several hundred contact binaries monitored in the framework of the program OGLE showed that the distribution of period variations of W UMa stars can be approximated by a normal distribution with an average

equal to zero and dispersion equal to 2.3×10^{-7} day/year (Kubiak et al. 2006). The observations are of very high accuracy but they are extended only over 13 seasons. The analysis of the observed period variations suggest that they have a random character with predominantly low values of \dot{P} resulting in time scales substantially longer than the stellar thermal time scale. Such a distribution excludes TRO as a primary source of the variations. A much more probable reason for the observed variations is connected with possible fluctuations of the mass transfer between the components. The stream flowing from the primary to the secondary and back carries $10^{-3} - 10^{-4} M_{\odot}$ /year. A relative fluctuation of this flux at the level of $10^{-3} - 10^{-4}$ can produce the observed period variations. Fluctuations of that order are expected as a result of magnetic activity cycles operating on W UMa stars (Applegate 1992). The existence of activity cycles have been suggested from the analysis of a long-time photometric behavior of heavily spotted stars. The average magnitude of those stars varies on time scales of several decades. This would be the expected time scale of period variations in contact binaries.

The present model of large scale circulations supplements the evolutionary model of W UMa type stars in which contact binaries are past mass exchange with mass ratio reversal (Stępień 2004, 2006a,b) i. e. they are in an evolutionary state similar to low mass Algols. The basic difference between W UMa type stars and low mass Algols is that the latter stars have more orbital AM and longer periods so only the secondary fills its Roche lobe. Binaries with lower orbital AM form contact binaries in which the overflow of the critical equipotential surface by both components drives large scale circulations encircling the whole secondary and a large fraction the primary. Matter transported by the circulations to the secondary (with the mass flux of the order of $10^{-3} - 10^{-4} M_{\odot}$ /year) returns back to the primary but a fraction of thermal energy associated with that matter is radiated away during the flow around the secondary. It was argued that the expected flow velocities attain a substantial fraction of the sound velocity. Such values were assumed when considering details of the flow. To determine an accurate value of the flow velocity numerical hydrodynamic simulations are needed. Particularly important in this respect is the fate of the returning flow. If it behaves like a waterfall, the expected flow velocities can be close to sound velocity. If, instead, it collides with the primary's matter so that the high pressure wave moves back along the flow, the driving force will be reduced and the flow velocity lowered.

REFERENCES

- Allen C.W., 1973, *Astrophysical Quantities*, 3rd ed., Athlone Press, London
- Applegate J.H., 1992, *ApJ*, 385, 621
- Baker N.H., Temesvary S., 1966, *Tables of Convective Stellar Envelopes*, 2nd edition, NASA, Washington
- Baran A., Zola S., Rucinski S. M., Kreiner J. M., Siwak M., Drozd M., 2004, *AcA*, 54, 195
- Bilir S., Karataş Y., Demircan O., Eker Z., 2005, *MNRAS*, 357, 497
- Binnendijk L., 1970, *Vistas in Astron.*, 12, 217
- Brown, B.P., Browning, M.K., Brun, A.S., Miesch, M.S., Toomre, J., 2008, *astro-ph0808.1716*
- Cruddace R.G., Dupree A.K., 1984, *ApJ*, 277, 263
- Cutispoto G., Messina S., Rodono M., 2003, *A&A*, 400, 659
- Eggleton P.P., 1996, in *The Origins, Evolutions, and Destinies of Binary Stars in Clusters*, eds. E.F. Milone, J. -C Mermilliod, *ASP Conf. Ser.*, Vol. 90, p. 257
- Eggleton P.P., Kiseleva L., 2001, *ApJ*, 562, 1012
- Flannery B.P., 1976 *ApJ*, 205, 217
- Gazeas K.D., Niarchos, P.G., Zola S., Kreiner, J.M., Rucinski S.M., 2006, *AcA*, 56, 127
- Gazeas K., Stępień K., 2008, *MNRAS*, 390, 1577
- Guinan E.F., Bratstreet D.H., 1988, in *Formation and Evolution of Low Mass Stars*, eds. A.K. Dupree, M.T.V.T. Lago, Dordrecht, Kluwer, p. 345
- Hazlehurst J., Refsdal S., 1978, *A&A*, 62,L9
- Innis J.L., Budding E., Oláh K., Järvinen S.P., Coates D.W., Messina S., Kaye T.G., 2008, *IBVS*, No. 5832
- Kähler H., 2004, *A&A*, 414, 317
- Kaluzny J., Rucinski S.M., 1993, in *Blue Stragglers*, ed. R.A. Saffer, *ASP Conf. Ser.*, Vol. 53, p. 164
- Kreiner, J.M., Kim, C.W., Nha, J.L., 2001, *An Atlas of O - C diagrams of eclipsing binary stars*, Wyd. Nauk. AP, Kraków
- Kubiak, M., Udalski, A., Szymański, M.K., 2006, *AcA*, 56, 253
- Kuiper G.P., 1941, *ApJ*, 93, 133
- Lipari S.L., Sistero R.F., 1988, *PASP*, 100, 377
- Lubow S.H., Shu F.H., 1975, *ApJ*, 198, 383
- Lubow S.H., Shu F.H., 1976, *ApJ*, 207, L53
- Lucy L.B., 1968, *ApJ*, 151, 1123
- Lucy L.B., 1976, *ApJ*, 205, 208
- Martin T.J., Davey S.C., 1995, *MNRAS*, 275, 31
- Mochnecki S.W., 1981, *ApJ*, 245, 65
- Mochnecki S.W., 1985, in *Interacting Binaries*, eds. P.P. Eggleton, J.E. Pringle, Dordrecht, Reidel, p. 51
- Oka K., Nagae T., Matsuda T., Fujiwara H., Boffin H.M.J., 2002, *A&A*, 394, 115
- Paczyński B., Sienkiewicz R., SzczygiełD.M., 2007, *MNRAS*, 378, 961
- Pribulla T., Chochol D., Heckert P.A., Errico L., Vittone A.A., Parimucha S., Teodorani M., 2001, *A&A*, 371, 997
- Pribulla T., Kreiner J.M., Tremko J., 2003, *Contr. Astr. Obs. Skalnaté Pleso*, 33, 38
- Pribulla T., Rucinski S.M., 2008, *MNRAS*, 386, 377
- Rasio F.A., 1995, *ApJ*, 444, L41
- Ritter H., Zhang Z.-Y., Kolb U., 2000, *A&A*, 360, 969
- Rucinski S.M., 1985, *MNRAS*, 215, 615
- Rucinski S.M., 1998, *AJ*, 116, 2998
- Rucinski S.M., 2000, *AJ*, 120, 319
- Rucinski S.M., 2002, *PASP*, 114, 1124
- Rucinski S.M., Duerbeck H.W., 1997, *PASP*, 109, 1340
- Rucinski S.M., Paczynski B., 2002, *IBVS*, No. 5321
- Rucinski S.M., Pribulla T., van Kerkwijk M.H., 2007, *AJ*, 134, 2353
- Sarna M.J., Fedorova A.V., 1989, *A&A*, 208, 111
- Shu F.H., Lubow S.H., Anderson L., 1976, *ApJ*, 209, 536
- Shu F.H., Lubow S.H., Anderson L., 1976, *ApJ*, 229, 223
- Spruit H.C., 1974, *Solar Physics*, 34, 277
- Spruit H.C., Weiss A., 1986, *A&A*, 166, 167
- Stępień K., 1995, *MNRAS*, 274, 1019
- Stępień K., 2004, in *Stars as Suns: Activity, Evolution and*

- Planets, IAU Symp. No. 219, eds. A.K. Dupree, A.O. Benz, Astr. Soc. of Pacific, p. 967
Stępień K., 2006a, *AcA*, 56, 199
Stępień K., 2006b, *AcA*, 56, 347
Stępień K., Schmitt J.H.M.M., Voges W., 2001, *A&A*, 370, 157
Tapia S., Whelan J.A., 1975, *ApJ*, 200, 98
Tassoul J.-L., 1992, *ApJ*, 389, 375
Vilhu O., 1982, *A&A*, 109, 17
Vilhu O., Walter F.M., 1987, *ApJ*, 321, 958
Webbink R.F., 1976, *ApJS*, 32, 583
Wolter U., Robrade J., Schmitt J.H.M.M., Ness J.U., 2008, *A&A*, 478, L11
Yakut K., Eggleton P.P., 2005, *ApJ*, 629, 1055